JACC: CARDIOVASCULAR INTERVENTIONS VOL. 5, NO. 6, 2012

ISSN 1936-8798/$36.00
PUBLISHED BY ELSEVIER INC. http://dx.doi.org/10.1016/j.jcin.2012.02.016

Computed Tomographic Angiography–Verified Plaque Characteristics and Slow-Flow Phenomenon During Percutaneous Coronary Intervention

Takahide Kodama, MD, PhD,* Takeshi Kondo, MD, PhD,* Akitsugu Oida, MD, PhD,* Shinichiro Fujimoto, MD, PhD,* Jagat Narula, MD, PhD†

Takasaki, Japan; and New York, New York

Objectives This study sought to identify whether computed tomographic angiographic (CTA) plaque characteristics are associated with slow-flow phenomenon (SF) during percutaneous coronary intervention (PCI).

Background SF during PCI is associated with myocardial damage and prolonged hospitalization. Intracoronary ultrasound–verified large echolucent lesions have been reported to predict SF.

Methods The authors evaluated pre-PCI CTA plaque characteristics in 40 consecutive patients (male/female, 31/9; age, 69 ± 10 years) with stable angina pectoris who developed SF during PCI; patients with ≥600 Agatston coronary artery calcium score were not included. They were compared with 40 age-, sex-, and culprit coronary artery–matched patients (male/female, 31/9; age, 69 ± 9 years) who underwent PCI during the same period and did not develop SF. Plaque characteristics, including vascular remodeling, plaque consistency, including low-attenuation plaques representing lipid-rich lesions and high-attenuation plaque patterns of calcium deposition, were analyzed.

Results Calcium deposition in the perimeter of a plaque, or circumferential plaque calcification (CPC), was significantly more frequent in the SF group (25 of 40, 63%) than the no-SF group (2 of 40, 5.0%) ($p < 0.001$). Presence of CPC on CTA was confirmed at the same location in the nonenhanced CT during Agatston coronary artery calcium score calculation. The positive remodeling index was significantly higher (1.5 [1.3 to 1.8] vs. 1.2 [1.0 to 1.5]; $p < 0.001$) and plaque density significantly lower (23.5 [9.5 to 40] HU vs. 45 [29 to 86] HU; $p = 0.001$) in the SF group. The conditional logistic regression analysis revealed that CPC, plaque density, and dyslipidemia were the predictors of SF, with CPC being the strongest (odds ratio: 79; 95% confidence interval: 8 to 783, $p < 0.0001$).

Conclusions CTA-verified CPC with low-attenuation plaque and positive remodeling were determinants of SF during PCI. If CTA findings are available in patients undergoing PCI, the interventionists should be aware of the likelihood of SF. (J Am Coll Cardiol Intv 2012;5:636–43) © 2012 by the American College of Cardiology Foundation

From the *Department of Cardiology, Takase Clinic, Takasaki, Japan; and the †Zena and Michael A. Weiner Cardiovascular Institute, Mount Sinai School of Medicine, New York, New York. The authors have reported that they have no relationships relevant to the contents of this paper to disclose.

Manuscript received December 29, 2011; accepted February 13, 2012.

The slow-flow (SF), or no-reflow phenomenon, has been frequently reported with percutaneous coronary intervention (PCI) procedures. SF is associated with elevated peripheral biomarkers of myocardial injury and less favorable clinical outcomes with prolonged hospital stay (1,2). Post-procedural SF in patients presenting with acute coronary syndromes is commonly associated with intravascular ultrasound (IVUS)-verified luminal thrombus load, large plaque

See page 644

burden, and echolucent plaques (3–5). Although the IVUS information is largely available from the patients with acute coronary syndrome, pre-procedural computed tomographic angiography (CTA) findings in a very small group of patients undergoing PCI for stable coronary disease have reported a possible association of lipid-rich low-attenuation plaque (LAP) with SF (6,7). It should be clinically useful to noninvasively identify a subset of patients prone to develop SF after an elective coronary interventional procedure. Since LAP likely represent lipid-rich necrotic cores of the target lesions (8), accurate information obtained noninvasively before PCI may allow either institution of medical therapy for possible plaque stabilization and postponement of procedure (9), or preparation for an appropriate distal protection device to prevent the post-procedural complication (10,11).

The present study was undertaken to identify CTA determinants, if any, of post-procedural SF during elective PCI in a large number of patients with stable angina pectoris in a retrospective pair-matched case-control study design.

Methods

Subjects. From April 2006 to June 2010, elective PCI was performed in 3,369 stable angina pectoris patients at our institute. Of these, 111 (3.3%) patients developed SF during PCI as defined by Thrombolysis In Myocardial Infarction (TIMI) flow grade 0 to 2 (12) as described later in the text. Of these 111 patients, coronary CT angiograms were available in 44 patients; CT angiograms were performed within 1 week of the PCI in 30 patients and within 2 months in the remaining. Of these 44 patients, 4 with an Agatston coronary artery calcium score (Agatston score) (13) ≥600 and/or unacceptable CT image quality were excluded, leaving 40 (male/female, 31/9; age, 69 ± 10 years) consecutive patients with post-PCI SF. CT angiographic characteristics from the SF patient group were compared with a control group of 40 age-(±2 years), sex-, and culprit coronary artery–matched patients (male/female, 31/9; age, 69 ± 9 years) identified by a blinded statistician. These 40 patients underwent PCI for stable angina pectoris during the same time period, had their CT angiograms within 2 month before the PCI procedure, and did not develop SF during the PCI.

Coronary 64- and 320-slice CT imaging protocol. Unless contraindicated, atenolol (25 mg) was administered orally on the night before the examination to the patients with a heart rate of more than 60 beats/min. Alternatively, 2 to 10 mg of propranolol, as indicated, was injected intravenously immediately before scanning to attain a low heart rate. We always considered prospective electrocardiogram (ECG) gating for the scan to reduce the radiation dose to as low as possible. CT angiographic imaging was performed either using a 64-slice CT scanner (Aquilion 64, Toshiba Medical Systems, Otawara, Japan, and BSM-2401 ECG monitor, Nihon Kohden, Tokyo, Japan), or a 320-slice CT scanner (Aquilion ONE V4.51, Toshiba Medical Systems and an IVY3000 ECG and Heart Rate Monitor, IVY Biomedical Systems, Branford, Connecticut). A dual-flow injector (Stellant, Nihon Medrad K.K., Osaka, Japan) was used for the contrast administration. The contrast medium injection time was fixed, and the injection rate and injection volume were determined according to the patient's weight.

Abbreviations and Acronyms

Agatston score = Agatston coronary artery calcium score
CI = confidence interval
cMPR = curved multiplanar reformat
CPC = circumferential plaque calcification
CTA = computed tomographic angiography
ECG = electrocardiogram
HU = Hounsfield units
IVUS = intravascular ultrasound
LAP = low-attenuation plaque
OR = odds ratio
PCI = percutaneous coronary intervention
SF = slow-flow phenomenon
TIMI = Thrombolysis In Myocardial Infarction

For 64-slice CT imaging, a 2-phase injection method was used: contrast medium, a 50:50 mixture of contrast medium and saline, and saline solution were injected via an antecubital vein. In the CT scanner, the plane for the bolus-tracking method was set to the 4-chamber view level, and the injection was started. After 8 s, bolus tracking was performed, and scanning was begun upon visually confirmed arrival of the contrast medium in the left ventricle. At the same time, a voice message instructing the patient to hold his or her breath was played, and cardiac scanning initiated. The scanning was performed at a tube voltage of 120 kV (for patients weighing <70 kg) or 135 kV (for patients weighing ≥70 kg), a tube current of 400 to 600 mA, a gantry rotation speed of 0.35, 0.375, 0.4, or 0.45 s/rotation, a helical pitch of 8.0 to 11.2 (beam pitch: 0.125 to 0.175), a scan slice thickness of 0.5 mm, 64 rows, an image slice thickness of 0.5 mm, and a reconstructed interval of 0.3 mm. After acquisition of images, a 3-dimensional workstation (Ziostation, Ziosoft, Tokyo, Japan) was used for Agatston score calculation, and to generate 3-dimensional (volume rendering) as also curved multiplanar reformat (cMPR) images. By contrast, for 320-slice CT scanner use, contrast medium injection was performed in a 2-phase injection method: contrast medium for 10 s and saline solution for 8 s. Scanning was performed at a tube voltage of

120 kV, a gantry rotation speed of 0.35, 0.375, or 0.4 s/rotation, a scan slice thickness of 0.5 mm, an image slice thickness of 0.5 mm, and a reconstructed interval of 0.25 mm. As for tube current, in ECG asynchronous volume scan plan, the mean tube current numbers were calculated with a SD of 19, using automatic exposure control function at the range of 40 mm in the cephalic direction from the inferior border of the periphery of the right coronary artery. When tube current reached the maximum, the mean tube current number was calculated in the same manner using the tube voltage at 135 kV. The imaging range was set up at the minimal range chosen from 200 row, 240 row, 256 row, 280 row, and 320 row by referring to nonenhanced CT images for Agatston score measurement.

CTA interpretation. For plaque detection, both cross-sectional and longitudinal cMPR images were analyzed. Coronary arteries were divided into 16 segments based on the recommendations of the American Heart Association (14). Coronary artery segments with a diameter of >2 mm were evaluated for the presence of plaques. All plaques were characterized for significant stenosis (% stenosis >50%), vessel remodeling (positive, negative, none), plaque consistency (low or intermediate attenuation), disposition of coronary calcification (spotty, moderate, severe, circumferential), and ulcer-like appearance. Scans were interpreted by 3 investigators with no knowledge of the PCI findings.

Definition of CT plaque characteristics. CTA plaque characteristics are described as follows.

VESSEL REMODELING. Coronary arterial remodeling was defined as a change in the vessel area at the plaque site in comparison with the reference segment set proximal to the lesion in a normal-appearing vessel segment (reference area), and a remodeling index was calculated. Manual inspection, in both cross section and longitudinal reconstruction, was used for defining the remodeling index (lesion area/reference area).

PLAQUE CONSISTENCY. On the cross-sectional cMPR images of the target lesion, a region of interest >5 pixels (0.36 × 0.36 mm) was placed on at least 5 randomly selected points within each plaque, and the lowest CT density was defined as the minimum plaque density. Less than 30 Hounsfield units (HU) plaque attenuation was referred to as LAP, which in our experience represents IVUS-verified lipid-rich necrotic cores (9); plaque attenuation between 30 and 150 HU (intermediate-attenuation plaques) represents fibrous plaques. A plaque density of >150 HU (high-attenuation plaques) is consistent with calcification, and is used as a cutoff point for calcification in enhanced CT scans. In the present study, we frequently observed higher attenuation in a ring-like peripheral disposition, and defined peripheral calcification as a "circumferential plaque calcification" (CPC) when: 1) plaque attenuation was >150 HU; 2) it was seen at the same location in the pre-enhanced CT; 3) when the circumferential spread occupied >180° of the vascular perimeter; and 4) when the longitudinal spread of the calcification occupied greater than one-third of the plaque length (Fig. 1).

Coronary angiography and intervention protocol. All patients were pre-treated with 200 mg of aspirin and received an intravenous bolus of unfractionated heparin to maintain a therapeutic activated clotting time over 250 s during the PCI. Coronary angiography was performed by a single-plane angiography system (INFX 8000V, Toshiba Medical Systems) at a frame rate of 15 frames/s. Intracoronary injection of contrast medium performed by the mechanical automated injector (ACIST CVi, Acist Medical Systems, Minneapolis, Minnesota) at a flow volume rate of 2.5 ml/s. The interventional procedure was performed by the femoral approach using a 7-F guiding catheter. Multiple projections were obtained after intracoronary nitrate injection. In almost all patients, direct stenting was performed. Predilation was performed when stent delivery was expected to be difficult, and post-dilation with a noncompliant balloon was carried out at the operator's discretion.

Patients received 2 to 6 mg of intracoronary nicorandil administration and aspiration when SF developed during the procedure; an intra-aortic balloon pump was needed for 4 (10%) patients. At the end of the procedure, TIMI flow grade 3 was obtained in all patients. Although 3 of 4 patients who required intra-aortic balloon pump placement developed myocardial injury (creatine phosphokinase >1,000 IU/l), all the participants were discharged within 2 weeks after the procedure and were alive at 30 days after the procedure. The plaque volume, lesion length, and interpolated reference vessel diameter were assessed by quantitative coronary angiography, and the stent diameter and balloon inflation pressure were recorded.

Definition of SF. Coronary angiograms were evaluated by 3 observers who were blinded to the coronary CTA findings. SF was defined as coronary flow with TIMI flow grade 0 to 2 (5–7) with >5-min duration of ST-segment elevation on the ECG during the procedure, except for flow-limiting dissection, spasm, thrombus, or residual stenosis (Fig. 2).

Statistical analyses. This study is designed as a retrospective pair-matched case-control study. Cases and controls were matched (1:1) on age (±2 years), sex, and culprit artery. All statistical analyses were performed using SPSS version 13.0 J for Windows (IBM, Armonk, New York). For continuous variables, when data were normally distributed, the Student *t* test was used to identify whether intergroup differences were significant, and the results were presented as the mean ± SD. By contrast, when data were skewed, Mann-Whitney *U* test was used, and the results were presented as median and interquartile range. For discrete variables, the chi-square-test, or when the cell frequency was <5, the Fisher exact test was used to test significance. Conditional multivariate logistic regression analysis was used to provide adjusted odds ratio (OR) estimates for relation to slow-flow.

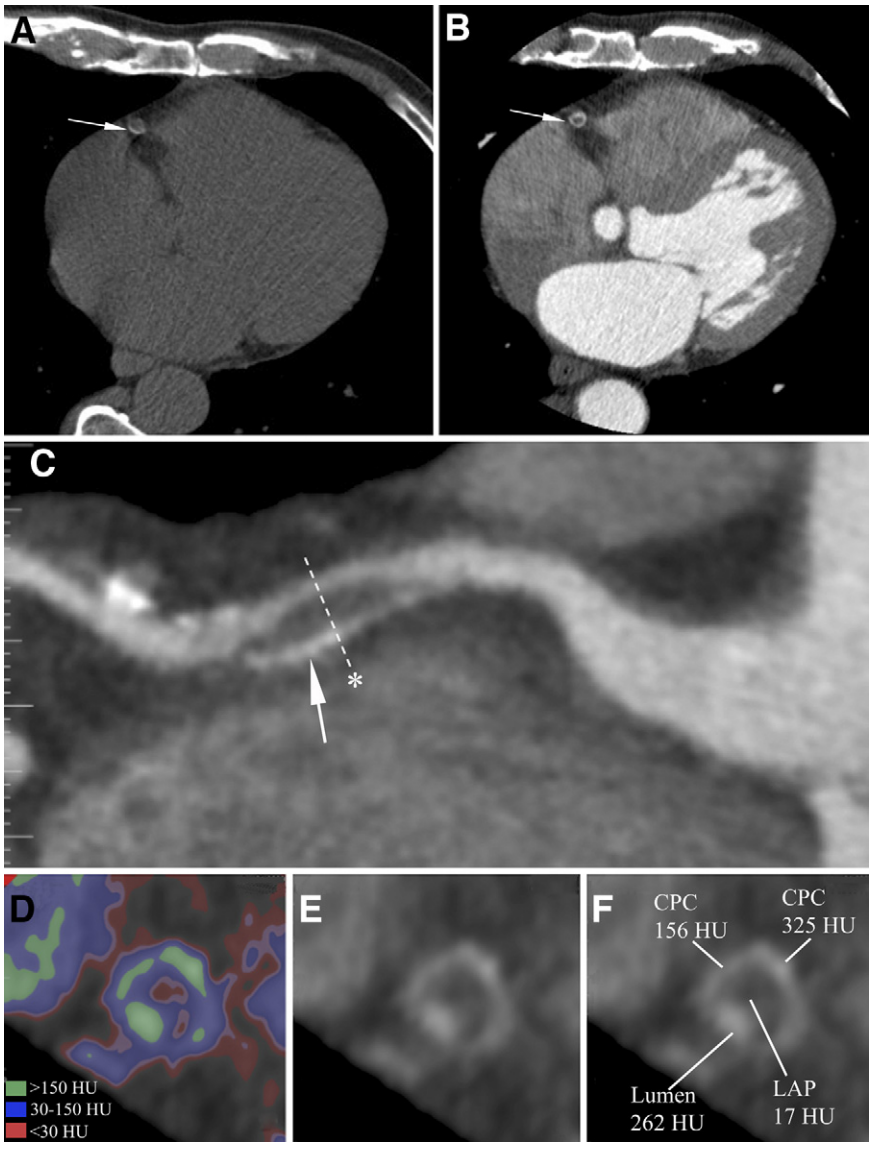

Figure 1. CTA Findings in a Patient Who Subsequently Developed SF During PCI

A ring-like calcification in the proximal segment of the right coronary artery (RCA) was observed on nonenhancement computed tomographic angiography (CTA) for coronary artery calcium scoring **(A)**. On an enhanced CT image at the same position as A, a similar ring-like calcification was found **(B)**. On a curved planar reconstruction image of the RCA, a big mixed plaque with positive remodeling and circumferential plaque calcification (CPC) **(arrow) (C)** is seen. Axial images sliced where indicated by the **line at the asterisk in C** are shown in **D, E, and F**. **(D)** shows a color map of the plaque based on CT Hounsfield unit (HU) values. A low-attenuation plaque (LAP) (17 HU) surrounded by CPC **(E and F)** is observed. PCI = percutaneous coronary intervention; SF = slow-flow phenomenon.

Results

Patient characteristics. Both the SF and control groups of patients were well matched (Table 1). There were no significant differences in age, sex, body mass index, hypertension, smoking, diabetes mellitus, stroke, family history, and serum creatinine level between the SF and control groups. However, presence of dyslipidemia in the SF group was more frequently observed than in the control group ($p = 0.019$); there was no significant difference in culprit vessels between the SF and control groups (Table 1).

CTA Determinants of SF. PRE-PROCEDURAL CT ANGIOGRAPHIC DETERMINANTS OF SF. The positive remodeling index was significantly higher (1.5 [1.3 to 1.8] vs. 1.2 [1.0 to 1.5], $p < 0.001$) and plaque density was significantly lower (23.5 [9.5 to 40] HU vs. 45 [29 to 86] HU, $p = 0.001$) in the SF group. The presence of CPC was significantly more frequent in the SF group (25 of 40; 63%) than in the control

Figure 2. Angiographic Outcome in the Same Patient

With the exception of **B,** all the still angiograms were obtained at the 20th frames after the contrast medium was injected into RCA. On a pre-procedural angiogram, the culprit lesion was in the proximal RCA **(arrows, A)**. Stent (Driver stent [Medtronic, Minneapolis, Minnesota]: 3.5 × 24 mm, inflation pressure: 12 atm) was deployed **(B)**. Slow-flow phenomenon developed with dramatic ST-segment elevation on electrocardiography and with severe chest pain **(C)**. Even after using intracoronary injection of nicorandil (4 mg) and an aspiration device, it was difficult to achieve Thrombolysis In Myocardial Infarction (TIMI) flow grade 3. An intra-aortic balloon pump was inserted **(arrowheads)** with resolution of ST-segment elevation and restoration of TIMI flow grade 3 **(D)**.

group (2 of 40; 5.0%) ($p < 0.001$). Ulcer-like appearance was not different between the control (5 of 40; 13%) and SF (4 of 40; 10%) groups ($p = 1.00$). Similarly, % stenosis was not different between the control and SF groups (69 ± 12% vs. 69 ± 11%, $p = 0.95$) (Table 1). CTA characteristics associated with SF were further analyzed by conditional multivariate logistic regression analysis. The positive remodeling index, CPC, minimum CT value, % stenosis, and dyslipidemia were included in analysis for conditional multivariate logistic regression analysis. CPC (OR: 79, 95% confidence interval [CI]: 8 to 783, $p < 0.0001$), the minimum CT value of plaque (OR: 0.977 for per unit decrease, 95% CI: 0.959 to 0.995, $p = 0.013$) and presence of dyslipidemia (OR: 18, 95% CI: 1 to 300, $p = 0.041$) emerged as the independent predictors of SF. The remodeling index did not emerge as an independent predictor of SF upon multivariable regression analysis (Table 2).

PROCEDURAL DETERMINANTS OF SF. The reference vessel diameter, the plaque volume, the lesion length, the last balloon size, and the last inflation pressure were also added to the list of variables to identify any additional features during PCI that may have influenced the procedural outcome. The reference vessel diameter (3.0 ± 0.7 mm vs. 3.2 ± 0.6 mm, $p = 0.19$), the plaque volume (61 ± 45 mm^3 vs. 69 ± 40 mm^3, $p = 0.19$), the lesion length (24 [18 to 30] mm vs. 18 [18 to 24] mm, $p = 0.19$), the last balloon size (3.5 [3.0 to 3.9] mm vs. 3.5 [3.0 to 3.5] mm, $p = 0.74$), and the last inflation pressure (13 [12 to 18] atm vs. 14 [12 to 16] atm, $p = 0.27$) were not significantly different between the control and SF groups (Table 1). All pre-procedural and procedural parameters were included for conditional multivariate logistic regression analysis, and the CPC (OR: 109, 95% CI: 10 to 1,202, $p < 0.0001$), the minimum CT value (OR: 0.976, 95% CI: 0.956 to 0.996, $p = 0.017$), presence of dyslipidemia (OR: 21, 95% CI: 1.5 to 294, $p = 0.024$), and the last inflation pressure (OR: 1.2, 95% CI: 1.016 to 1.533, $p = 0.035$) emerged as significant independent predictors of SF (Table 2).

Discussion

In the present study, we found the CPC surrounding a region of LAP was the important determinant of the SF associated with a PCI procedure for stable coronary disease.

Table 1. Baseline Characteristics, CCTA Findings, and Procedural Variables

Variable	All Patients (N = 80)	Control Group (n = 40)	SF Group (n = 40)	p Value
Age, yrs	69 ± 9	69 ± 9	69 ± 10	NS
Male	62 (78)	31 (78)	31 (78)	NS
BMI	24.2 ± 3.2	24.1 ± 3.1	24.3 ± 3.4	NS
Medical history				
Hypertension	57 (71)	30 (75)	27 (73)	NS
Dyslipidemia	66 (83)	29 (73)	37 (93)	0.019
Smoking	19 (24)	10 (25)	9 (23)	NS
Diabetes mellitus	25 (31)	11 (28)	14 (35)	NS
Cerebral infarction	8 (10)	4 (10)	4 (10)	NS
Family history of IHD	19 (24)	9 (23)	10 (25)	NS
Serum creatinine, mg/dl	0.89 ± 0.27	0.86 ± 0.22	0.92 ± 0.11	NS
Culprit vessel				
LMT	2 (3)	1 (3)	1 (3)	NS
LAD	40 (50)	21 (53)	19 (48)	
LCX	10 (13)	6 (15)	4 (10)	
RCA	28 (35)	12 (30)	16 (40)	
CCTA findings				
Positive remodeling index	1.4 (1.2–1.6)	1.2 (1.0–1.5)	1.5 (1.3–1.8)	<0.001
Minimum CT value, HU	34 (18–75)	45 (29–86)	23.5 (9.5–40)	0.001
% Stenosis	69 ± 11	69 ± 12	69 ± 11	NS
CPC	27 (34)	2 (5)	25 (63)	<0.001
ULA	9 (11)	5 (13)	4 (10)	NS
Procedural variables				
Reference vessel diameter, mm	3.1 ± 0.6	3.0 ± 0.7	3.2 ± 0.6	NS
Plaque volume, mm^3	65 ± 43	61 ± 45	69 ± 40	NS
Lesion length, mm	20.5 (18–24)	24 (18–30)	18 (18–24)	NS
Last balloon size, mm	3.5 (3.0–3.5)	3.5 (3.0–3.9)	3.5 (3.0–3.5)	NS
Last inflation pressure, atm	14 (12–16)	13 (12–18)	14 (12–16)	NS

Values are mean ± SD, n (N), or median (interquartile range).

BMI = body mass index; CCTA = coronary computed tomographic angiography; CPC = circumferential plaque calcification; HU = Hounsfield Unit; IHD = ischemic heart disease; LAD = left anterior descending coronary artery; LCX = left circumflex coronary artery; LMT = left main trunk; NS = not significant; RCA = right coronary artery; SF = slow-flow phenomenon; ULA = ulcer-like appearance.

SF is associated with increased days of hospitalization, post-procedural myocardial infarction, and poor intermediate-term clinical outcomes (1,15,16), and it has been proposed that precise plaque assessment by IVUS before the PCI might be useful for the prediction of transient SF (3–5,17–20). Although IVUS has higher spatial resolution, it cannot detect signal behind dense calcification, and the IVUS information only becomes available during the procedure.

Table 2. Conditional Multivariate Logistic Regression Analysis for Determinants of Pre-Procedural and Procedural SF Phenomenon

	Odds Ratio	95% Confidence Interval	p Value
Pre-procedural variables			
CPC	79	8–783	<0.0001
Minimum CT value, HU	0.977	0.959–0.995	0.013
Dyslipidemia	18	1–300	0.041
Procedural variables			
CPC	108	10–1,202	<0.0001
Minimum CT value, HU	0.976	0.956–0.996	0.017
Dyslipidemia	21	1.5–294	0.024
Last inflation pressure, atm	1.2	1.016–1.533	0.035

Abbreviations as in Table 1.

However, since it has now become possible to evaluate the coronary plaque characteristics by multislice CT angiographic examination, it should be possible to identify the lesions that are more likely to be associated with SF and procedural complications. Although CT angiographic examination may miss small areas of calcification (21), it allows assessment of vascular segment (positive) remodeling, extent of calcification, and the plaque consistency in terms of attenuation characteristics (22–26). Kinohira et al. (6), in 4 subjects, demonstrated that a LAP (<50 HU, representing IVUS-verified lipid-rich lesion) detected by CTA was an important predictor of SF during PCI procedure. In 9 subjects, Nakazawa et al. (7) reported that the CT density of plaque was lower in patients with transient no-reflow during PCI as compared with those without transient no-reflow. Moreover, greater circumferential extent of the lipid-rich core on the cross-sectional CTA images, also described as a "napkin-ring" sign (27,28) of LAP, was more frequently observed in patients with SF. It is not likely that the lesions subjected to elective PCI for stable angina will be associated with significant thrombus burden. However, it is possible that a LAP, after the PCI, will spill lipid core contents in the downstream vessel segments, as has been recently demonstrated by near infrared spectroscopy (28–30).

In the present study, we observed that the lower-attenuation areas of the plaques resulting in SF are usually surrounded by a higher-attenuation plaque rim. Although the inner LAP area was necessary for the SF, attenuation did not always have to be lower than 30 HU as reported earlier by Motoyama and colleagues (31) for the plaques likely to result in major adverse coronary events spontaneously over time; the median consistency of the fateful plaques in our current study was 23.5 (9.5 to 40) HU. In addition, the higher-attenuation area surrounding the lower-attenuation area was extensive and needed to cover at least 2 quadrants in circumference and one-third of the longitudinal extent of the plaque. We termed such a rim of higher-attenuation plaque as CPC, which was observed in two-thirds of the subjects developing SF during PCI. Pre-enhanced CT data were available in 14 of 29 cases showing CPC, and circumferential high-density area could clearly be seen in 12 of 14 cases, which confirmed that the peripheral high attenuation did not result from simple contrast enhancement (28).

A lipid-rich plaque with a thin cap could easily disrupt upon balloon expansion, and could lead to release of lipid contents and cellular debris in the distal circulation. Even if a thick fibrous cap covered the lipid core, it is conceivable that a relatively noncompliant vessel due to CPC could increase intraplaque pressure during balloon inflation with consequent embolic complication. Indeed, the last inflation pressure during the interventional procedure was associated with SF complication. If the relationship between plaque characteristics and SF is established, it may not be unreasonable to defer procedure for statin treatment and plaque stabilization (9,32) or employ an appropriate distal protection device (10,11).

Study limitations. This study represents a single-center experience with a limited number of patients. Because the study design was a retrospective case-control study, inherent selection bias could not be excluded. Although we confirmed SF by TIMI flow grade deterioration and ST-segment elevation on ECG, we could not show precisely objective data of SF because of the lack of measurement of TIMI frame count or TIMI myocardial perfusion grade. Moreover, we only measured periprocedural enzyme release in patients who needed an intra-aortic balloon pump; therefore, we could not make a comparative study of the impact of SF on myocardial damage between patients with and without SF.

Conclusions

Although an LAP has been associated with SF during PCI, we observed that the CTA-verified LAP was often surrounded circumferentially by a CPC. If confirmed in larger prospective studies, it should become easier to develop protective and preventive strategies.

Acknowledgment
The authors thank Dr. Shinya Suzuki for statistical review of the manuscript.

Reprint requests and correspondence: Dr. Takahide Kodama, Department of Cardiology, Takase Clinic, 885-2 Minami-orui, Takasaki 370–0036, Japan. E-mail: kodama-tk@umin.ac.jp.

REFERENCES

1. Ramírez-Moreno A, Cardenal R, Pera C, et al. Predictors and prognostic value of myocardial injury following stent implantation. Int J Cardiol 2004;97:193–8.
2. Mehta RH, Harjai KJ, Boura J, et al. Prognostic significance of transient no-reflow during primary percutaneous coronary intervention for ST-elevation acute myocardial infarction. Am J Cardiol 2003;92:1445–7.
3. Okura H, Taguchi H, Kubo T, et al. Atherosclerotic plaque with ultrasonic attenuation affects coronary reflow and infarct size in patients with acute coronary syndrome: an intravascular ultrasound study. Circ J 2007;71:648–53.
4. Hong YJ, Jeong MH, Choi YH, et al. Impact of plaque components on no-reflow phenomenon after stent deployment in patients with acute coronary syndrome: a virtual histology-intravascular ultrasound analysis. Eur Heart J 2011;32:2059–66.
5. Iijima R, Shinji H, Ikeda N, et al. Comparison of coronary arterial finding by intravascular ultrasound in patients with "transient no-reflow" versus "reflow" during percutaneous coronary intervention in acute coronary syndrome. Am J Cardiol 2006;97:29–33.
6. Kinohira Y, Akutsu Y, Li HL, et al. Coronary arterial plaque characterized by multislice computed tomography predicts complications following coronary intervention. Int Heart J 2007;48:25–33.
7. Nakazawa G, Tanabe K, Onuma Y, et al. Efficacy of culprit plaque assessment by 64-slice multidetector computed tomography to predict

transient no-reflow phenomenon during percutaneous coronary intervention. Am Heart J 2008;155:1150–7.
8. Motoyama S, Kondo T, Anno H, et al. Atherosclerotic plaque characterization by 0.5-mm-slice multislice computed tomographic imaging. Circ J 2007;71:363–6.
9. Boden WE, O'Rourke RA, Teo KK, et al., for the COURAGE Trial Research Group. Optimal medical therapy with or without PCI for stable coronary disease. N Engl J Med 2007;356:1503–16.
10. Baim DS, Wahr D, George B, et al. Randomized trial of a distal protection device during percutaneous intervention of saphenous vein aorto-coronary bypass grafts. Circulation 2002;105:1285–90.
11. Ito N, Nanto S, Doi Y, et al. Distal protection during primary coronary intervention can preserve the index of microcirculatory resistance in patients with acute anterior ST-segment elevation myocardial infarction. Circ J 2011;75:94–8.
12. Sheehan FH, Braunwald E, Canner P, et al. The effect of intravenous thrombolytic therapy on left ventricular function: a report on tissue-type plasminogen activator and streptokinase from the Thrombolysis in Myocardial Infarction (TIMI Phase I) trial. Circulation 1987;75:817–29.
13. Agatston AS, Janowitz WR, Hildner FJ, Zusmer NR, Viamonte M, Detrano R. Quantification of coronary artery calcium using ultrafast computed tomography. J Am Coll Cardiol 1990;15:827–32.
14. Austen WG, Edwards JE, Frye RL, et al. A reporting system on patients evaluated for coronary artery disease. Report of the ad hoc committee for grading of Coronary Artery Disease, Council on Cardiovascular Surgery, American Heart Association. Circulation 1975;51:5–40.
15. Resnic FS, Wainstein M, Lee MK, et al. No-reflow is an independent predictor of death and myocardial infarction after percutaneous coronary intervention. Am Heart J 2003;145:42–6.
16. Yip HK, Chen MC, Chang HW, et al. Angiographic morphologic features of infarct-related arteries and timely reperfusion in acute myocardial infarction: predictors of slow-flow and no-reflow phenomenon. Chest 2002;122:1322–32.
17. Imoto K, Hiro T, Fujii T, et al. Longitudinal structural determinants of atherosclerotic plaque vulnerability: a computational analysis of stress distribution using vessel models and three-dimensional intravascular ultrasound imaging. J Am Coll Cardiol 2005;46:1507–15.
18. Lee SY, Mintz GS, Kim SY, et al. Attenuated plaque detected by intravascular ultrasound: clinical, angiographic, and morphologic features and post-percutaneous coronary intervention complications in patients with acute coronary syndromes. J Am Coll Cardiol Intv 2009;2:65–72.
19. Bayturan O, Tuzcu EM, Nicholls SJ, et al. Attenuated plaque at nonculprit lesions in patients enrolled in intravascular ultrasound atherosclerosis progression trials. J Am Coll Cardiol Intv 2009;2:672–8.
20. Wu X, Maehara A, Mintz GS, et al. Virtual histology intravascular ultrasound analysis of non-culprit attenuated plaques detected by grayscale intravascular ultrasound in patients with acute coronary syndromes. Am J Cardiol 2010;105:48–53.
21. van der Giessen AG, Gijsen FJ, Wentzel JJ, et al. Small coronary calcifications are not detectable by 64-slice contrast enhanced computed tomography. Int J Cardiovasc Imaging 2011;27:143–52.
22. Schroeder S, Kopp AF, Baumbach A, et al. Noninvasive detection and evaluation of atherosclerotic coronary plaques with multislice computed tomography. J Am Coll Cardiol 2001;37:1430–5.
23. Estes JM, Quist WC, Gerfo FW, Castello P. Noninvasive characterization of plaque morphology using helical computed tomography. J Cardiovasc Surg 1998;39:527–34.
24. Cordeiro MA, Lima JA. Atherosclerotic plaque characterization by multidetector row computed tomography angiography. J Am Coll Cardiol 2006;47 Suppl:C40–7.
25. Achenbach S, Moselewski F, Ropers D, et al. Detection of calcified and noncalcified coronary atherosclerotic plaque by contrast-enhanced, submillimeter multidetector spiral computed tomography: a segment-based comparison with intravascular ultrasound. Circulation 2004;109:14–7.
26. Leber AW, Becker A, Knez A, et al. Accuracy of 64-slice computed tomography to classify and quantify plaque volumes in the proximal coronary system: a comparative study using intravascular ultrasound. J Am Coll Cardiol 2006;47:672–7.
27. Narula J, Achenbach S. Napkin-ring necrotic cores: defining circumferential extent of necrotic cores in unstable plaques. J Am Coll Cardiol Img 2009;2:1436–8.
28. Maurovich-Horvat P, Hoffmann U, Corpahl M, et al. The napkin-ring sign: CT signature of high-risk coronary plaques? J Am Coll Cardiol Img 2010;3:440–4.
29. Goldstein JA, Grins C, Fischell T, et al. Coronary embolization following balloon dilation of lipid-core plaques. J Am Coll Cardiol Img 2009;2:1420–4.
30. Goldstein JA, Maini B, Dixon SR, et al. Detection of lipid-core plaques by intracoronary near-infrared spectroscopy identifies high risk of periprocedural myocardial infarction. Circ Cardiovasc Interv 2011;4:429–37.
31. Motoyama S, Sarai M, Harigaya H, et al. Computed tomographic angiography characteristics of atherosclerotic plaques subsequently resulting in acute coronary syndrome. J Am Coll Cardiol 2009;54:49–57.
32. Inoue K, Motoyama S, Sarai M, et al. Serial coronary CT angiography-verified changes in plaque characteristics as an end point: evaluation of effect of statin intervention. J Am Coll Cardiol Img 2010;3:691–8.

Key Words: circumferential plaque calcification (CPC) ■ CT angiography ■ slow-flow phenomenon.